Available online at www.sciencedirect.com

SciVerse ScienceDirect

Procedia Engineering 41 (2012) 281 – 288

Engineering Procedia

www.elsevier.com/locate/procedia

International Symposium on Robotics and Intelligent Sensors 2012 (IRIS 2012)

Novel Air-float Tactile Array for Stiffness Characterization in Soft Tissue Palpation

Indika B. Wanninayake[a,]*, Kaspar Althoefer[a], Lakmal D. Seneviratne[a,b]

[a]*King's College London, WC2R 2LS, London, U.K.*
[b]*Khalifa University of Science, Technology and Research, Abu Dhabi, U.A.E.*

Abstract

This paper presents a feasibility study of a novel air-float palpation probe for stiffness characterization in soft tissues. The probe is designed to accommodate multiple sensing elements which allow rapid acquisition and averaging of tactile information. Each sensing element has a sphere floating on a thin lubricating film of air. Hence the probe can move over soft tissues in any direction in a near frictionless manner. With the air pressure maintained constant, the displacement of each sensing element is a direct function of the stiffness of the tissue under investigation. The sensor has a tunable force range and the indentation force can be adjusted externally to match tissue limitations. The structure, working principle, a mathematical model for sensor output and the behavior of the tactile sensing system are described.

Keywords: Tactile Sensing; Optical Sensing , Haptics and Haptic Interfaces

1. Introduction

Minimally Invasive Surgical techniques benefit the patient because of reduced tissue trauma, minimal scarring, faster recovery, shorter hospital stay and reduction of intra operative blood loss. These surgeries are performed using specially designed tools inserted through small incisions of approximately 10-15mm diameter. Although MIS is widely used as the standard-of-care for some surgeries, it has not been adopted for many complex surgical procedures. This is mainly due to significant technical drawbacks encountered currently, including lack of direct hand-eye coordination, limited dexterity, lack of 3D visualization, poor ergonomic design and lack of haptic feedback. The application of robotics to MIS has taken the field into a new era. Especially, the advances in robotic-assisted surgical systems such as the da Vinci™ (Intuitive surgical Inc [1]), have helped to overcome most of the aforementioned disadvantages. The advantages offered by these surgical systems include enhanced 3D vision, high distal dexterity with 7 degree of freedom, motion scaling, tremor reductions as well as natural hand-eye alignment at the surgical console. However, the lack of haptic feedback still remains as a major drawback of systems currently in clinical use.

Haptic is a broad term used to describe both tactile (cutaneous) and force (kinesthetic) information needed to simulate the sensation felt by the hand. Of the two types, the tactile information which is readily available in an open surgery is very useful in identifying tissue abnormalities and hidden pathological lesions such as tumors. As most of the tumors tend to be harder than the surrounding tissue [2], tactile information can be used to indicate the presence, location and size of the

* Indika B. Wanninayake. Tel.: +44-208-547-8610
E-mail address: w.wanninayake@kingston.ac.uk

1877-7058 © 2012 Published by Elsevier Ltd. Open access under CC BY-NC-ND license.
doi:10.1016/j.proeng.2012.07.174

tumors, thereby enhancing the chance of performing a successful surgery. Additionally, the force information is vital in assessing the tool tissue-interaction in order to avoid damage to healthy soft tissue as it differentiates harder tissues. Therefore the aim of this paper is to present the findings of a feasibility study of a tactile probe which will serve as an extension to the surgeon's finger in order to carry out palpation during MIS.

2. Literature survey

Unlike in general robotic applications more stringent requirements are necessary in medical applications such as MIS. Hence, further advancement in force and tactile sensing methods are vital for developing acceptable tools and instruments to re-establish the required haptic feedback. Specifications for such tools can vary from application to application. However, some guidelines for developing tools for MIS specific applications are available in Table 1, [3]-[6].

Table 1. Desired specifications for tactile sensors in MIS,

MIS Application	Force Range	Sensitivity	Size (mm)	Other common Requirements
Endoscopic Grasper	±10N	0.2	≤15mm	Biocompatibility
Palpation Tool	0-2N	0.01	≤15mm	Sterilizability
Needle Driver	±2.5N	0.01	≤15mm	Lightweight
Air-float Probe	0-4N Variable	0.008	18	water-proof cost effective

A number of tactile sensors developed for tissue characterization and identification of abnormalities have been reported in [6]-[12]. In 2004, Ottermo et al. [6] have developed a surgical instrument which can act as an extended finger to perform tasks of palpation. The instrument has an end effector with a piezoelectric tactile sensor array. The sensor array is 24mm x 8mm in size and consists of 30, Pz27 piezoceramic piezoelectric elements. The sensing elements have been designed for a mean force of 10N. When in contact, the instrument can detect variation of tissue stiffness within the localized area. Another interesting approach to tissue differentiation is reported in [7]. Uribe et al. used piezoelectric bimorph to extract tactile information. The bimorph has two piezoelectric layers, for actuating and sensing respectively. The ac voltage supplied to the actuator vibrates the bimorph near resonant frequency. When in contact with the tissues the shift in frequency and the amplitude is used to differentiate various tissue properties. A palpation instrument based on capacitive mode of transduction was reported in [8]. In this study, the sensor array has 64 sensing elements and can measure forces between 0-2N with a resolution of 0.001N. Although, all the above discussed tactile sensors have proven their capability to identify tissue abnormalities, they can only measure the tissue stiffness variation within a very small area at a time. Moving over tissues to scan a larger area is impossible with those methods due to high frictional forces which could damage the sensor as well as sensitive tissue. In 2008, Liu et al. [9] developed a new tactile probe based on a force sensitive wheel. Fast acquisition of tactile information is possible with this method as the wheel can roll over the tissue covering a larger area in a short time. Here, the wheel-tissue interaction forces are measured using a commercially available ATI Nano17 sensor. Although the sensor can measure forces in 3 degree of freedom (DOF), indentation depth information is not available with this sensing method. Hence it should be used in conjunction with an indentation depth sensor for soft tissue characterization. Mechanical complexity and the increased size due to the Nano17 force sensor are some other drawbacks of this method. A tactile sensor which has overcome most of the aforementioned disadvantages has been developed by Zbyszewski et al [10]. Force sensing is based on relating the movement of the sphere against the pressure of air to a modulation of light intensity measured by optical fibers. The sensor is used to identify tissue abnormalities. The lubricating air film and the existence of the sphere at the probe tip allow the probe to move in any direction over the tissues to acquire tactile information. However, with a single sphere, covering a large area is difficult and time consuming due to the limited contact area. In view of the limitations associated with the above tactile sensing methods, a new developed tactile probe based on the above principle for tissue abnormality identification is discussed here. The modified probe uses spheres with 4mm diameter for each sensing element providing a better sensitivity for tissue characterization. Further, the array of the sensing element could be used to improve the accuracy of the measurement system through averaging and also it helps to cover a larger area in a limited time.

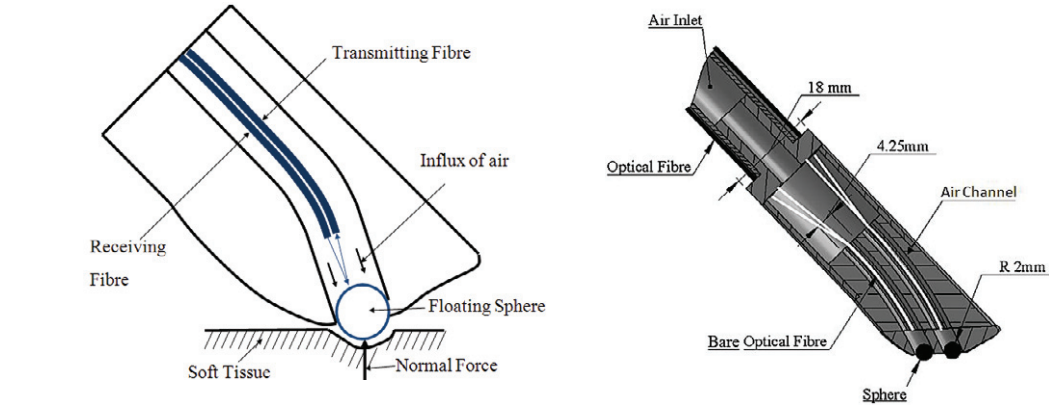

Fig.1. (a) Schematic diagram explaining the working principle of the proposed sensor (b) Longitudinal cross-section of the air-float probe

3. Design and the principle of operation of the Air-float Probe

3.1. Principle of operation

The proposed tactile sensing probe is designed to be used as a palpation tool for identification and visualization of tissue abnormalities. The principle of measurement that is used is extrinsic light intensity modulation of optical fiber. The tactile array consists of four sensing elements. Each sensing element has a sphere which is held at the end of a circular tunnel by a steady flow of air, as illustrated in Fig.1 (a). The sphere is free to rotate in all directions and can move into the channel when pressed against the airflow. When rolling over tissue, the displacement of the sphere, which is dependent upon the stiffness of the scanned tissue, is picked up by the optical fiber just above it. Optical intensity variation in each sensing element is used to characterize and identify tissue stiffness variations. Force applied by each sensing element on the tissue is a function of the air pressure supplied to the probe. Hence, changing air pressure allows the examination of tissue at different indentation forces. This method of tissue characterization has several advantages over conventional methods, such as near frictionless rolling over tissues, rapid acquisition of tactile information, high frequency response and lack of hysteresis. Most of all, the sensitivity of the tactile array can be adjusted by varying air pressure to suit different MIS applications.

3.2. Design

The sensor array consist of four optical displacement sensing elements of 4mm diameter each and are arranged in a 2x2 pattern, leading to an overall sensing area of 10 mm x 10mm. These sensing elements are equally spaced and mounted on the tip of the proposed tactile probe. A longitudinal cross section of the prototype probe is shown in Fig.1. (b). The outer diameter of the probe is 18 mm and made up of three main components which are conjoined using adhesives. The outer part and the middle part of the probe have four 4.25mm tunnels to accommodate optical fiber cables, spheres and allow the influx of air. The diameter of each tunnel gradually narrows down to 3.8mm at the tip of the probe to stop the sphere moving out of the tunnel. Brackets with an inner diameter of 1mm are incorporated in the design to support and guide the optical fibers whose tips are placed 5mm away from the tip of the probe. The inner hollow part of the probe has eight 2.2mm diameter holes to accommodate the fiber cables and a 10mm diameter extension for the air inlet. The prototype was made out of ABS plastic and was build up using a 3D rapid prototyping machine (Dimension 768) which has a minimum layer resolution of 0.245mm. Plastic optical fibers of 980/1000 - µm core/cladding diameter and 0.47 numerical aperture are used in a parallel configuration to measure the motion of the spheres. Optical photoelectric switches (E3X-DA- N Series, OMRON Europe B.V) combined with a 1 kHz low pass filter are used as the optical detection circuit. A 16 bit data acquisition (DAQ) module (NI- USB 6211) and the LabViewTM 8.0 software package are used to acquire the measured signals. The sampling rate is 100Hz.

4. Mathematical model for the voltage- displacement characteristics of the tactile sensor

With the air flow supplied to the probe is maintained at a constant rate, the force exerted by each sensing element on the tissue is nearly constant. Hence the displacement of the spheres can directly be related to the stiffness of the scanned tissue. As the displacement of the sphere is measured through the optical system, sensitivity of the system depends on the optical intensity distribution of the reflected light beam. An analytical formula for the spatial intensity distribution of reflected light can be formulated by considering the geometry of the optical components. As illustrated in Fig.2. (a), the geometry of the system is defined in Cartesian coordinate system. A spherical reflector with radius of curvature a is centered at the origin and a transmitting optical fiber with a diameter of D is placed at a distance d away from the center. Another fiber cable with a diameter D is placed parallel to the transmitting fiber and is used to collect reflected light and delivers it to an optical detector.

It is assumed that the light beam projected onto the reflector is highly collimated with a Gaussian form of intensity distribution profile so the wavefronts are nearly planar. However, at the surface of the reflector, the incoming planar wavefronts are transformed into spherical wavefronts and advances along the z-axis. The dashed lines and dotted curves transverse to the z-axis indicate the wavefronts of transmitted and reflected beams. As schematically indicated, the reflected spherical wavefronts appears as if they are originated from a virtual source placed behind the reflector. Hence the spatial intensity distribution of the reflected beam is derived by considering a virtual transmitting fiber placed at the focal point of the reflector which emits Gaussian spherical wavefronts in the z direction. The beam expands with a constant cone angle θ.

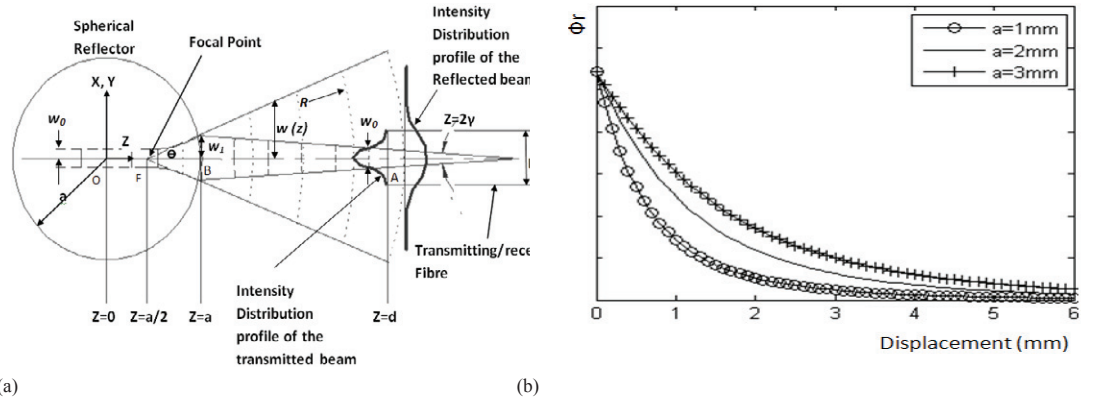

Fig.2. (a) Geometry of the optical intensity modulation system using a spherical reflector (b) Simulated reflective power intensity at the receiving optical fiber for varying reflector positions. (for three different reflector radius a=1mm, 2mm, 3mm) Model constants, w_0=0.4mm, γ=0.65 rad

As the reflected beam propagates only in z direction, characteristics of the spherical Gaussian beam can be derived using paraxial approximation [11], a spherical wave is approximated to a planar wave propagating nearly parallel to the z. In order for this approximation to be valid the point of observation should be restricted to a point near the axis of propagation. For a spherical Gaussian beam, the Electric field intensity distribution across a plane, transverse to the direction of propagation can be written as [12]

$$E(x,y,z,t) = E_{0(Z)}\, e^{\frac{ik(x^2+y^2)}{2\,R(z)}}\, e^{-\frac{(x^2+y^2)}{w(z)^2}}\, e^{i(kz-\omega t)}, \tag{1}$$

where,

$E_{0(Z)}$- the electric field intensity at the centre of the beam,

$R(z)$ - the radius of curvature of the beam wavefront,

$w(z)$ - the Gaussian beam's half- width at $1/e$ of the peak.

ω - the angular frequency and,

$k = \frac{2\pi}{\lambda}$, Where λ is the spectral wavelength of the source.

Since the beam irradiance is proportional to the square of the electric field amplitude, total power of the beam can be obtained by evaluating the integral,

$$\emptyset_{tot} = \iint_A |E(x,y,z,t)|^2 \, dA = [E_0(z)]^2 \int_0^\infty e^{\frac{-2r^2}{w^2}} 2\pi r dr \; = [E_0(z)]^2 \; \frac{\pi[w(z)]^2}{2}. \tag{2}$$

At the transmitting end of the optical fiber $E_0(z)$ and $w(z)$ are E_0 and w_0 respectively. Using equation (2), the total power emitted out of the virtual fiber can be written as

$$\emptyset_{tot} = {E_0}^2 \, \frac{\pi {w_0}^2}{2} \tag{3}$$

As the wave progresses, total emitted power remains the same, but the spot size of the Gaussian beam increases, resulting in a decrease of the maximum power intensity at the centre of the projected light beam. Using equation (2) and (3), Variation of maximum power intensity at the centre of the beam and the change in the width of the transmitted beam can be written as

$$E_0(z) = \frac{E_0 w_0}{w(z)}, \tag{4}$$

$$w(z) = \; w_0 + (d - z) \; tan\, \gamma. \tag{5}$$

Here, γ is the divergence angle of the light beam. Using equation (5), Gaussian width at the surface of the reflector can be estimated as

$$w_1 = \; w_0 + (d - a) \; tan\, \gamma. \tag{6}$$

The reflected beam expands with a constant cone angle θ in the near field. However, θ is a function of w_1 and varies as per the distance between the transmitting fiber and the reflector. Hence, variation of the beam expansion angle and the Gaussian width can be derived as

$$tan\, \theta = \frac{w_1}{FB} = 2w_1/a, \tag{7}$$

$$w(z) = \; w_0 + \left(Z - \frac{a}{2}\right) tan\, \theta \tag{8}$$

Using equation (2), reflected power passing through a circular aperture of diameter D can be written as

$$\emptyset_r = [E_0(z)]^2 \int_0^{D/2} e^{\frac{-2r^2}{w(z)^2}} 2\pi r \, dr \tag{9}$$

Evaluating the integral and substituting for$E_0(z)$ and $w(z)$, the theoretical formula for the optical power collected at the receiving fiber can be written as

$$\emptyset_r = \frac{\pi {E_0}^2 {w_0}^2}{2} \left(1 - e^{\left[\frac{-2(\frac{D}{2})^2}{(w_0 + \frac{2(w_0 + (z-a)\, tan\, \gamma)}{a}\left(z - \frac{a}{2}\right))^2}\right]}\right). \tag{10}$$

Using the theoretical model derived, optical power intensity variation at the receiving fiber for different reflector positions is simulated and plotted against the reflector displacement (see Fig.2. (b)). It is evident from the simulation that the gradient of the response curves increases with decreasing reflector diameter. A higher sensitivity could be achieved by selecting a sphere with a smaller diameter for each sensing element. However, the effective range of the response curve decreases as the diameter decreases thus relatively a lower displacement is achievable for small sphere sizes. The mathematical model derived here is validated against the experimental data later in this paper under section 5).

5. Performance Analysis of the sensor

5.1. voltage-displacement characteristics

Initially, to investigate the voltage-displacement characteristics of the four displacement sensing elements, the prototype probe was attached to the distal tip of a Mitsubishi RV-6SL, a 6-DOF (Degree of Freedom) robotic manipulator, to allow accurate motion control. The distal end of the prototype was connected to an air compressor. The compressor was turned on to generate a steady flow of air and the air pressure was adjusted to 0.1bar, which is equivalent to 10kPa. The sensor array was positioned onto a flat surface by lowering the robot arm, with only the tip of the spheres touching the surface. The spheres were gradually intended into their tunnels by lowering the robot arm in 0.1mm steps. The maximum displacement achieved was 1.1mm. The displacement and corresponding signal from each sensing element were recorded.

The results of the experiment are encouraging as all four sensing elements show a clear variation of output voltage against the sphere displacement (see Fig.3. (b)). With the resolution of 0.2mV at the optical detector, displacement of the spheres can be detected to the level of 0.008mm. Theoretical response curve derived for a 4mm diameter reflector also indicated in each figure using a solid line. It is clear from the graphs that there exist a very good correlation between the theoretical model and the experimental data. The RMSE for d_1,d_2, d_3 and d_4 were 0.033, 0.020, 0.021 and 0.054. However, further work will be necessary to improve the repeatability and the linearity of the sensor.

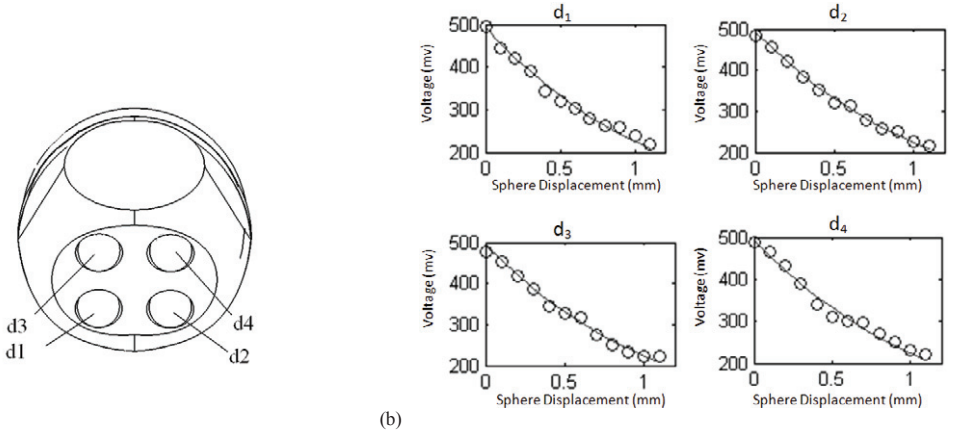

(a) (b)

Fig.3. (a) Element identification (b). Characteristics of each element (Experimental data and the theoretical response curve)

5.2. Force Range

This experiment was carried out in order to investigate force-pressure characteristics of the sensor array. The prototype was connected to the distal tip of the Mitsubishi RV-6SL and the sensor array was navigated to the ATI Mini40 force sensor rigidly mounted to a work bench and then the robot arm was lowered until only the tips of the spheres were touching the force sensor. The air pressure was initially adjusted to 0.05bar (5kpa) and then the robot arm was further advanced towards the force sensor by 0.1mm. Then air pressure was increased up to 100kPa in 5kPa steps and data from the Mini40 was collected using a 16bit data acquisition card (NI PCI 6013). Force information collected is sampled, averaged and then plotted against the air pressure as shown in Fig.4. According to Fig.4 (a), the force available at the sensing element increases with the supply air pressure. This is considered being a very important feature of this sensing method. The force applied by the sensor can be adjusted externally to match the sensitivity requirements of the tissue of various internal organs.

5.3. Interaction between sensing elements

Since all the sensing elements are connected to the same air supply, displacement of one sensing element could affect the sensitivity of the whole sensor array. Hence, the purpose of the next experiment was to investigate the variation of force available, at each sensing element due to the displacement of the others. To achieve this, the sensor array was navigated to a ATI Mini40 force sensor in such a way that only one sensing element (d_1) make contact with the force sensor. Then the prototype was further advanced towards the force sensor to get displacement of 0.5mm at sphere d1. The air pressure was adjusted to 100kPa. Keeping the robot arm stationary, the other three spheres are intended into their channels, one at a time

at a constant rate and the data from the Mini40 was collected using a 16bit data acquisition card (NI PCI 6013). The same experiment was repeated and data was collected for two spheres, and the three spheres moving in simultaneously at a constant rate. Data for each stage is averaged and then plotted against sphere displacement as shown in Fig.4 (b).

From the information presented in Fig.4 (b), it is clear that the force available at any sensing element is directly affected by the displacement of the other elements within the array. The Force, 0.5N available at d1 drops down to 0.42N when one other sphere is intended into its channel and it is further drops to 0.32N when all the three spheres are intended in. This is due to the decrease in air pressure inside the probe, as the flow rate increases due to the opening of more channels. However, if the scanning started with all the spheres intended into their channels halfway, variation of displacements between the spheres would have a minimum effect on the others as the curves are almost flat after the initial 0.2mm displacement. Effect would be significant only if one or more spheres extended out to reach a 0.2mm or a lesser displacement.

Another very important feature of this method is that if the pressure is maintained at constant, the force applied by the sensor is constant for any sphere displacement. Hence once the initial force is set by adjusting the air pressure, there is no fear of increasing it beyond this limit which could cause damage to the tissue under inspection. However, the initial force applied by the sensor, before sphere displacement started is slightly higher compared to the forces applied later. This is mainly due to the rise in air pressure inside the channel due to the closure of the exit by the sphere.

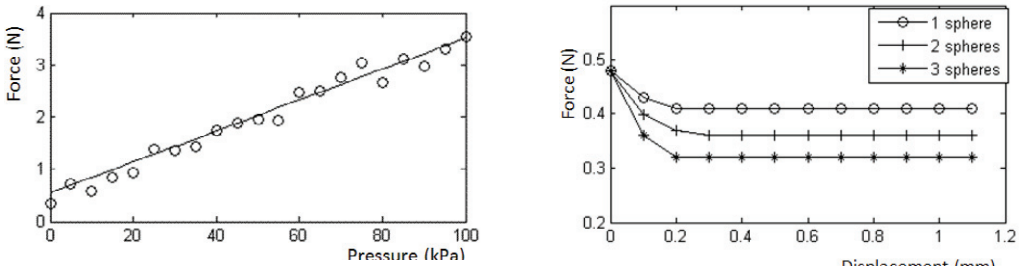

Fig.4. (a) Force – air pressure characteristics of the probe (b) Interactions between different sensing elements.

6. Discussion

The prototype probe discussed in this paper has been developed to evaluate the feasibility of using an air-float tactile sensor array to perform tissue abnormalities identification. Considering the results from the validation experiments, the sensor has the potential to measure indentation depth variations of a spherical indenter with a very high sensitivity. Further, it has a tunable force range and indentation force can be adjusted externally to match tissue limitations. Force range and the force displacement characteristics of the sensor are also promising for application relating to the MIS. The sensing technique being optical light intensity modulation enabling the use of non metallic components, the probe may be used in environments requiring MRI compatibility. However, as the supply air pressure has a direct impact on the sensitivity of the indenter, maintaining a steady airflow and a constant air pressure inside the probe is very important to ensure accuracy of measurements. Additionally, build up of air pressure within the channels may lead to excessive forces. Hence precise pressure regulation is a key element for correct functioning of this prototype. However, this could be challenging due to the dynamic nature of the open system. Further, the sensing method being optical light intensity modulation, factors such as variation of reflectivity of sphere due to dust and the fluids in contact, attenuation due to fiber bending, source light intensity variation and misalignment of fibers due to movement could potentially lessen the performance. The effects of these factors have not yet being evaluated and further work is being done to evaluate and model these interactions.

7. Conclusion

This paper presents a feasibility study of a novel tactile sensing probe for MIS. Initial validation experiments demonstrate that the developed sensor has the potential to measure indentation depth variations with a higher sensitivity. Indentation force can be set by adjusting the air pressure and when an initial force is set, it will never be exceeded regardless of the indentation. This prevents the sensor from exerting excessive forces that may damage the tissue as long as the initial force is set according to the tissue limitations. Additionally, the probe has the ability to move in any direction over the surface of a soft tissue organ to acquire tactile information rapidly in a near-frictionless manner. Further work aims at

improving the sensor fabrication quality and modeling the sensor behavior under variety of operating conditions. Further we aim to carry out ex-vivo and in-vivo trials to evaluate the sensors potential as a tactile probe to detect tissue abnormalities.

References

[1] G.S. Guthart, and J.K. Salisbury,"The Intuitive TM telesurgery system: Overview and application", Proc. IEEE Int Conf. Robotics and Automation, pp. 618-621, 2000.
[2] T.A. Krouskop, T.M. Wheeler, F. Kallel, B.S. Garra, and T. Hall, "Elastic moduli of breast and prostate tissues under compression," *Ultrason. Imaging,* vol. 20, pp. 260-274, 1998.
[3] J. Peirs, J. Clijnen, D. Reynaerts, H. Van Brussel, P. Herijgers, B. Corteville, and S. Boone, "A micro optical force sensor for force feedback during minimally invasive robotic surgery," Sensors and Actuators A, vol. 115, pp. 447-455, Sep. 2004
[4] M. Lazeroms, G. Villavicencio, W. Jongkind and G. Honderd,"Optical fiber force sensor for minimal-invasive surgery grasping instruments", Annual International Conference of the IEEE Engineering in Medicine and Biology Society, pp. 234–235., 1996
[5] G. L. McCreery, A. L. Trejos, M. D. Naish, R.V. Patel, and R. A. Malthaner,"Feasibility of locating tumours in lung via kinaesthetic feedback". Int. J. Med. Robot. Comput. Assist. Surg, Vol 4, pp. 58–68, 2008
[6] M.V. Ottermo, O. Stavdahl, and T.A.Johansen,"Palpation instrument for augmented minimally invasive surgery,"IEEE/RSJ International Conference on Intelligent Robots And Systems, vol.4, pp. 3960- 3964, sept 2004
[7] D.O.Uribe, R.Stroop, T.Hemsel, and J.Wallaschek ,"Development of a biomedical tissue differentiation system using piezoelectric actuators,"IEEE International Frequency Control Symposium, pp. 91 – 94, 2008
[8] R.D. Howe, W.J. Peine, D.A Kantarinis, and J.S. Son, "Remote Palpation Technology," IEEE Magazine in Medicine and Biology, vol. 14, no.3, pp. 318-323, may 1995
[9] H. Liu, et al. "The Rolling Approach for Soft Tissue modeling and Mechanical Imaging during robot-assisted Minimally Invasive Surgery" ,Proc. IEEE Int. Conf. Robot. Autom. ,pp. 846-850, 2008.
[10] D. Zbyszewski, P. Polygerinos, L.D Seneviratne, and K. Althoefer. , "A novel MRI compatible air-cushion tactile sensor for Minimally Invasive Surgery," IEEE/RSJ International Conference on Intelligent Robots and Systems, pp.2647-2652, Oct. 2009
[11] R. Guenther, Modern Optics, John Wiley, 1990, pp. 361-433.
[12] F.L Pedrotti, L.S. Pedrotti, Introduction to Optics. Prentice Hall, 1987, pp. 456-487.